Virchows Arch [Pathol Anat] (1986) 408:559–574

Virchows Archiv A

Time course of arterial repair following endothelial denudation in the rat carotid artery

A morphometric study in Wistar and Sprague-Dawley rats

Elizabeth van Pelt-Verkuil, Jan Knoester, Wilfrid van Pelt, Marijke Brink, Dick Jense, and Jef J. Emeis*

TNO Gaubius Institute for Cardiovascular Research, Herenstraat 5d, 2313 AD Leiden, The Netherlands

Summary. Repair processes in the intima and media of the rat carotid artery were studied morphometrically for time intervals of up to 28 days after injury induced by air-drying. Air-drying injury included endothelial denudation as well as medial necrosis.

Repair was most rapid between days 9 and 11 after injury as regards the increase in myointimal lesion size, the extent of repopulation of the media and re-endothelialization. After day 11, myointimal lesion size continued to increase until day 28. Medial repair, however, almost completely ceased at day 11, 25% of the inner media and 5% of the outer media remaining necrotic. At day 21, the vessels were almost completely re-endothelialized; however, even at day 28, about 10% of the middle of the vessel was still permeable to Evans Blue.

The response of Sprague Dawley rats to injury differed from that of Wistar rats. Compared with Wistar rats, Sprague Dawley rats showed larger myointimal lesions, less medial necrosis and slower endothelial repair. It is suggested that the extent of medial necrosis and the speed of endothelial regeneration affect the arteriosclerotic response in rats

Key words: Endothelial denudation – Medial necrosis – Arteriosclerosis – Rat – Carotid artery

Introduction

Experimental endothelial denudation leads to proliferation and migration of smooth muscle cells (SMCs), indicating that these events are relevant to the pathogenesis of arteriosclerosis (Thorgeirsson and Robertson 1978; Ross and Glomset 1973, 1976; Ross 1981). Ideally, in animal models aimed at specific injury to the endothelium, the media should remain unaffected

Offprint requests to: J.J. Emeis's present address:* Laboratory School Rijnland, Leidse Dreef, 2352 BA Leiderdorp, The Netherlands

(Hirsch and Robertson 1977; Karnovsky 1981). Medial necrosis, however, occurs to some extent in almost all animal models aimed at selective endothelial denudation of large areas of the vessel wall (Bondjers and Björnheden 1970; Schwartz et al. 1975; Haudenschild et al. 1981; Van Pelt-Verkuil et al. 1983). Myointimal lesion development is inhibited in rabbit aorta homografts deprived of SMCs (Spaet et al. 1975), in mechanically injured rat aorta (Poole et al. 1971) and in rabbit aorta near necrotic areas (Björkerud and Bondjers 1971). In the latter case, lesions developed only adjacent to normal, undamaged media. A small amount of medial necrosis presumably interferes with the extent of myointimal thickening, as suggested by our own studies (Van Pelt-Verkuil et al. 1983) and those of Hassler (1970), both in rat carotid arteries. Even slight damage to the subendothelium might influence endothelial repair and arteriosclerotic lesion development in certain species (Reidy et al. 1982).

Although the size and/or shape of the denuded area is a major factor in determining the extent of the arteriosclerotic response (Clowes et al. 1976; Haudenschild and Schwartz 1979; Falcone et al. 1980), medial necrosis thus also influences the reaction of the arterial wall to endothelial injury.

Medial repair, i.e. repopulation of the media by SMCs, has been shown to occur in the rat carotid artery after mechanical injury and feezing (Hassler 1970) and in the rabbit aorta after superficial longitudinal trauma (Björkerud and Bondjers 1973). In our previous experiments using air-drying injury of the Wistar rat carotid artery endothelium, medial necrosis involving large areas of the denuded arterial segment was observed. As medial necrosis was less extensive at day 14 than at day 1, repair processes in the media also occur in this animal model. The present study was aimed at following the time course of medial repair, myointimal lesion development and endothelial repair for 28 days after air-drying. Special attention was paid to the extent of repair at day 14, the time at which the arteriosclerotic response is normally evaluated in this model (Clowes et al. 1976; Guyton et al. 1980; Van Pelt-Verkuil et al. 1983) and to the effect of medial necrosis on myointimal thickening.

As pilot studies had shown that Sprague Dawley (SD) rats had less medial necrosis but considerably larger lesions than Wistar (Wi) rats, the myointimal lesions, media necrosis and endothelial repair of SD rats at day 14 were compared with the data on Wi rats obtained at days 14 and 28.

Materials and methods

Surgical procedure and tissue processing. Experimental arteriosclerosis was induced in the carotid artery of male Wistar rats (Wi) (weighing 350–400 g) using a modification of Fishman's air-drying method (Fishman et al. 1975; Van Pelt-Verkuil et al. 1983), an air-flow rate of 28 ml/min being applied for 4 min. Animals were killed at 5 ($n=7$), 7 ($n=6$), 9 ($n=7$), 11 ($n=9$), 14 ($n=24$), 21 ($n=7$) and 28 ($n=13$) days after injury. After i.v. injection of Evans Blue, the carotid arteries were perfusion-fixed at 130 cm water pressure with 1-ethyl-3,3-(diaminopropylcarbodiimide) and embedded in paraplast. The vessel wall morphology was evaluated by means of morphometry of 6 μ thick serial cross-sections at 125 μ intervals along

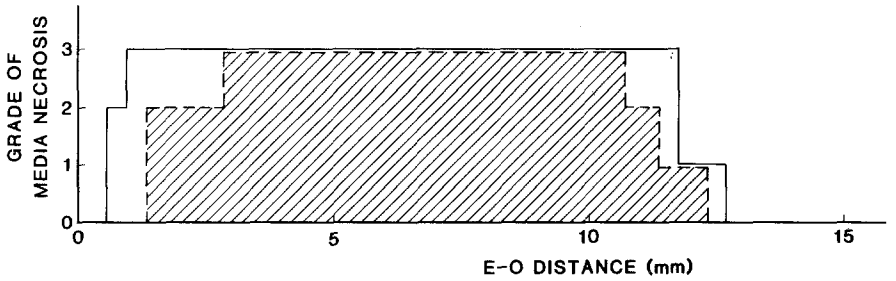

Fig. 1. Graphical presentation of medial necrosis along the vessel wall (EO distance) at day 5 after air-drying. The intensity of medial necrosis was graded in three (discontinuous) classes of injury for the inner (———), as well as for the outer (– – – –) medial layer. The begin and endpoint of each grade of necrosis (grade 1,0%–33%; grade 2, 33%–66%; grade 3, 66%–100% of the media devoid of SMC nuclei) was determined from sections. The *shaded area* is an example of a volume measure (% of outer medial necrosis)

the entire denuded carotid artery segment, which were stained by the Elastic-van Gieson procedure as described earlier (Van Pelt-Verkuil et al. 1983). Experimental arteriosclerosis was also induced in ♂ SD rats ($n=15$) of the same age and weight exactly as described for Wi rats and evaluated at day 14 after endothelial denudation.

Morphometry. Variables describing the myointimal lesion and endothelial repair were determined as described elsewhere in detail (Van Pelt-Verkuil et al. (1983)). In brief, the *myointimal lesion* was characterized by: begin (proximal) and end (distal) point, total length, maximal thickness, percentage of the intimal surface covered by the lesion, and by a measure of lesion volume (cf Fig. 7 in Van Pelt-Verkuil et al. 1983). *Endothelial repair* was assessed by assessing the following variables: complete re-endothelialization, partial re-endothelialization (showing local platelet adherence in cross-sections), and absence of endothelialization. In addition, the area still permeable to Evans Blue was determined macroscopically. The begin and end points of these zones and their lengths were determined.

Variables describing *medial necrosis* (i.e., the absense of SMCs) were determined separately for the inner an outer medial layers. The inner medial layer was defined by the elastica interna and the second elastic lamella. The remainder of the media comprised the outer medial layer. The severity of medial necrosis was graded as 1, 2 or 3, corresponding to necrosis of, respectively, 0%–33%, 33%–66% and 66%–100% of the vessel circumference. The begin and end points of these grades were measured. These data were graphed by plotting the begin and end points on the X-axis and the severity of necrosis by grade 1, 2 or 3 on the Y-axis (Fig. 1). They were read by means of a digitizer tablet yielding a continuous series of Y-values (i.e., the intensity of medial necrosis). To compare individual patterns of necrosis, the graphs were transformed by dividing the X-axis into 50 equidistant points and finding the corresponding Y-values. These Y-values, considered as homologous for each individual, were used to calculate the mean pattern of necrosis grade for each of the X-values along the denuded artery segment. The total percentage of necrosis as a volume measure was determined for each individual rat by calculating in the digitized graph the area representing necrosis along the air flow entry-outflow (EO) distance (Fig. 1, shaded parts for outer media necrosis). This area was divided by the area found in the case of maximal necrosis (score 3) along the entire EO distance and multiplied by 100. Total length of necrosis grade 1, 2 or 3 was calculated from begin and end point coordinates (cf Fig. 3).

Statistical analysis. Differences between Wi and SD rats were evaluated by univariate analysis (Van Pelt-Verkuil et al. 1983) using all variables at day 14 and those of Wi rats at day 28. Depending on the number of groups, we used either Student's T-test or one-way analysis of variance after testing for normality and equality of variances. If these criteria were not met, Kruskall-Wallis' test was used.

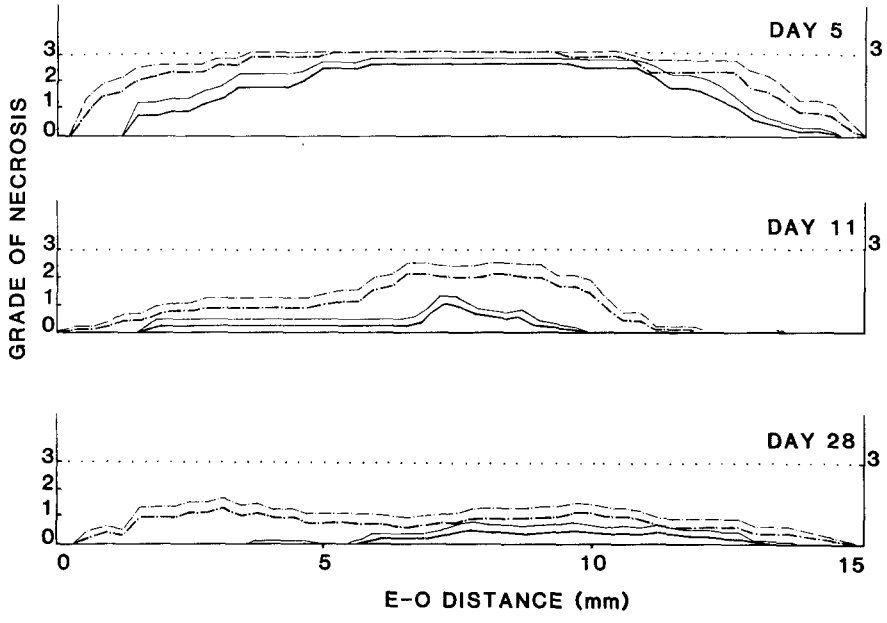

Fig. 2. Graphical presentation of mean grade of medial necrosis (+SEM) of the inner (–·–·–) and outer (———) medial layer(s) along the vessel wall segment at days 5, 11 and 28 after air-drying. Maximal score of necrosis is represented by the *dotted line* at grade 3. Due to the determination of mean values, the Y-values now represent a continuous series of data

Results

Repair of necrotic media (Figs. 2, 3; Table 1; cf. Fig. 5)

Medial necrosis is present in large areas of both the inner (75.6%) and the outer (51,6%) media at day 5 after endothelial denudation (Table 1). Extensive necrosis is found in the middle part of the vessel in both inner and outer media.

A gradual repair of inner medial necrosis takes place up to day 9. The length of the necrotic areas of grade 1, 2 and 3 as well as the percentage of necrosis diminishes (Fig. 3A; Table 1). The most affected areas are located in the proximity of the inflow hole of air and in the middle part (cf. Fig. 5 for day 7), whereas the media regains its normal morphology distally.

The most extensive repair occurs between days 9 and 11 (cf. Figs. 3, 6 inset; Table 1). Some additional repair takes place up to day 28, but the differences do not reach significance if day 11 is compared with day 28. The pattern of necrosis, however, becomes more diffuse and in general does not exceed grade 1 (Fig. 2).

Apart from slight differences, the repair of outer media necrosis is very similar to that of the inner media. The total percentage of necrosis decreases, whereas the variables describing the length of the various grades of necrosis also become smaller (Fig. 3B). Outer medial necrosis also recovers most

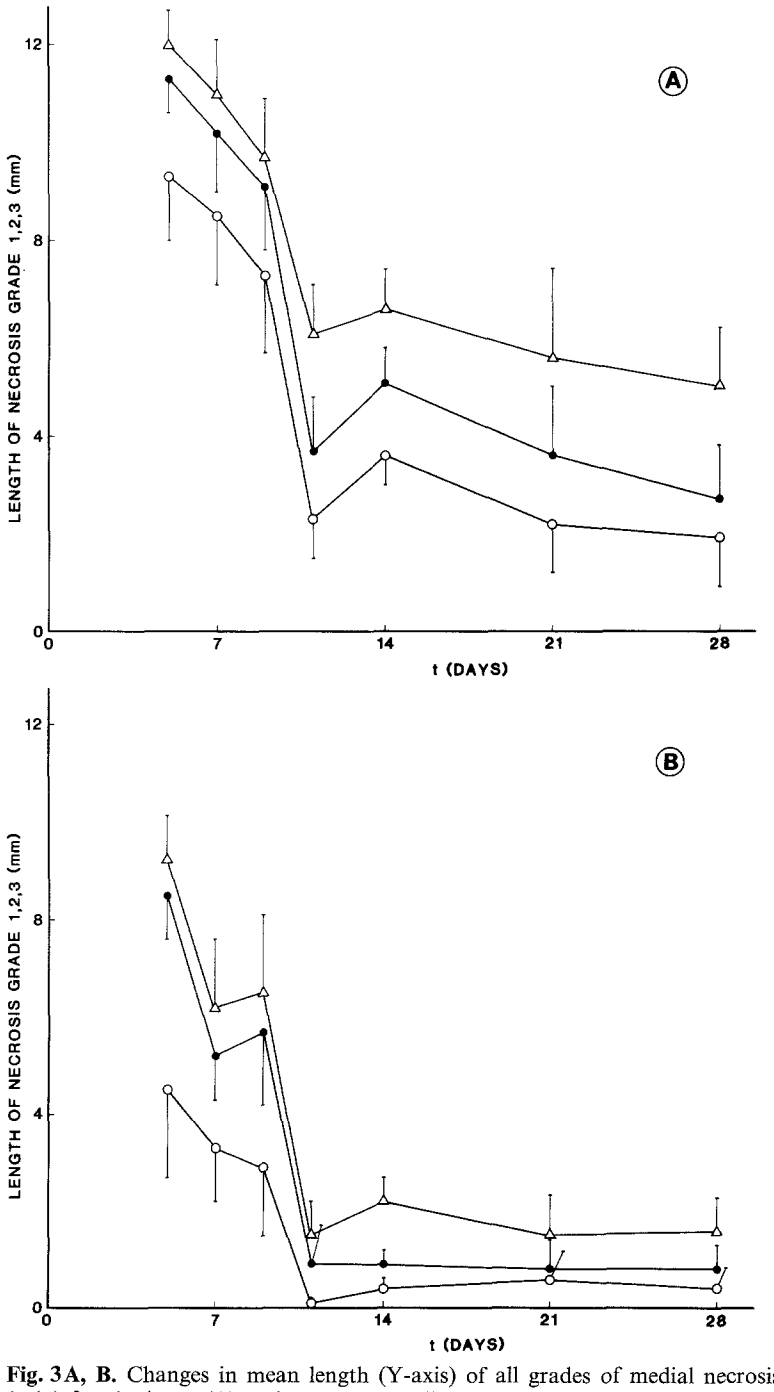

Fig. 3A, B. Changes in mean length (Y-axis) of all grades of medial necrosis 1, (△); 2, (●); 3, (○) for the inner (**A**) and outer (**B**) medial layers. These length measures were determined by subtracting proximal from distal positions for the three necrosis grades for each individual at each time sampling point from day 5 up to day 28 after air-drying induced endothelial denudation (X-axis)

Table 1. Changes in the mean total percentage of necrosis in the inner and outer media (as a volume measure) for each time point from day 5 upt to day 28 after air-drying induced endothelial denudation in Wistar rats

	Percentage of necrosis (±SEM)	
	Inner	Outer
day 5	75.8±5.0	51.6± 7.2
7	68.3±7.5	33.0± 6.7
9	61.8±9.8	36.3±10.6
11	28.3±5.8	5.7± 3.3
14	32.3±4.3	7.0± 1.9
21	26.0±9.2	6.8± 4.2
28	22.1±6.8	6.3± 3.5

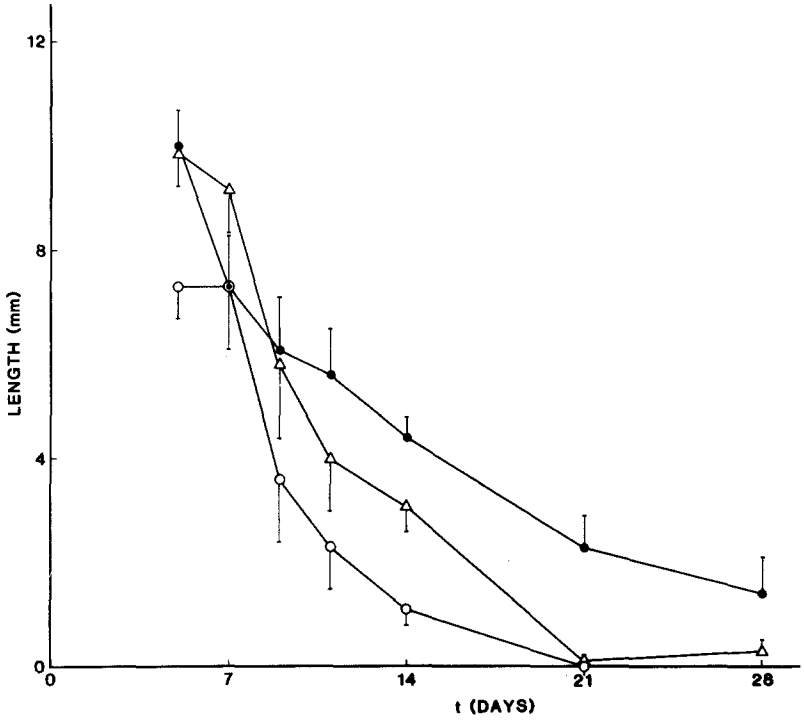

Fig. 4. Repair of endothelial lining from day 5 up to day 28 after endothelial denudation by air-drying injury, describing: **a** Length of intima still fully denuded (○), completely covered with platelets. **b** Length of still partially denuded intima (△), covered with platelets. **c** Length of the vessel wall still permeable to Evans Blue (●)

extensively between days 9 and 11. Grade 3 necrosis has almost disappeared at day 28, while grades 1 and 2 only remain present in the middle of the vessel wall (Fig. 2). No significant repair is found between day 11 and 28.

Repair of endothelial lining (Fig. 4)

Endothelial repair takes place gradually during the 4 week period after air-drying, endothelial cells covering the layer of deposited platelets. No differ-

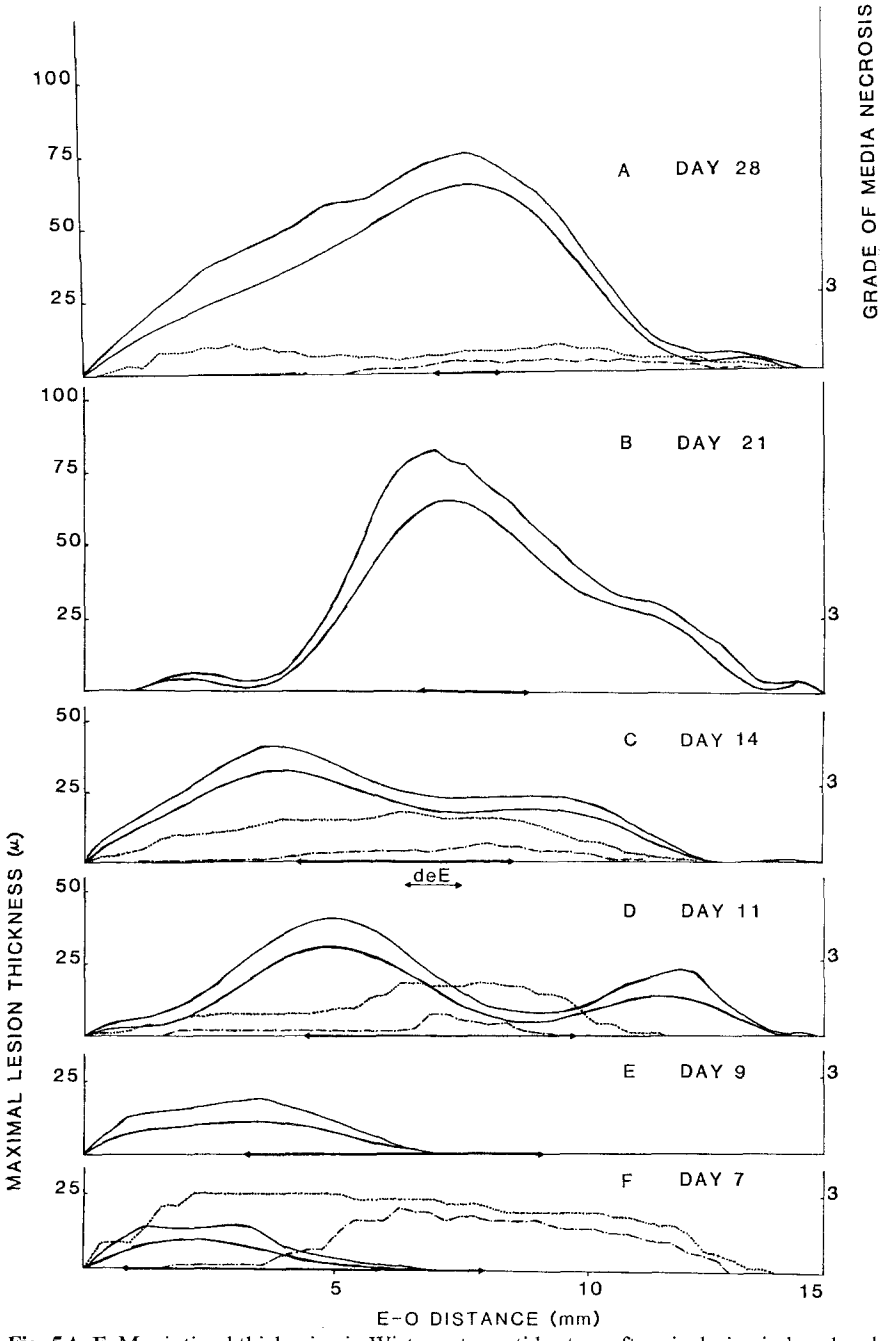

Fig. 5A–F. Myointimal thickening in Wistar rat carotid artery after air-drying induced endothelial denudation. Best fit of myointimal lesion thickness (*drawn line*) (+SEM) along the damaged artery segment (EO) as described by a 10th degree polynomal for each of the time sampling points. These curves were generated in a similar way from the maximal intimal thickening patterns of individual rats measured along the EO distance as described for medial necrosis. To compare the myointimal thickening patterns with the intesity of media damage, the mean scores of the inner (.....) and outer (–·–·–) medial necrosis are given for sampling at days 7, 11, 14 and 28. The *heavy line* marked on the X-axis indicates the localization of Evans Blue permeation. At day 14, the position of the still fully denuded vessel wall is indicated by deE

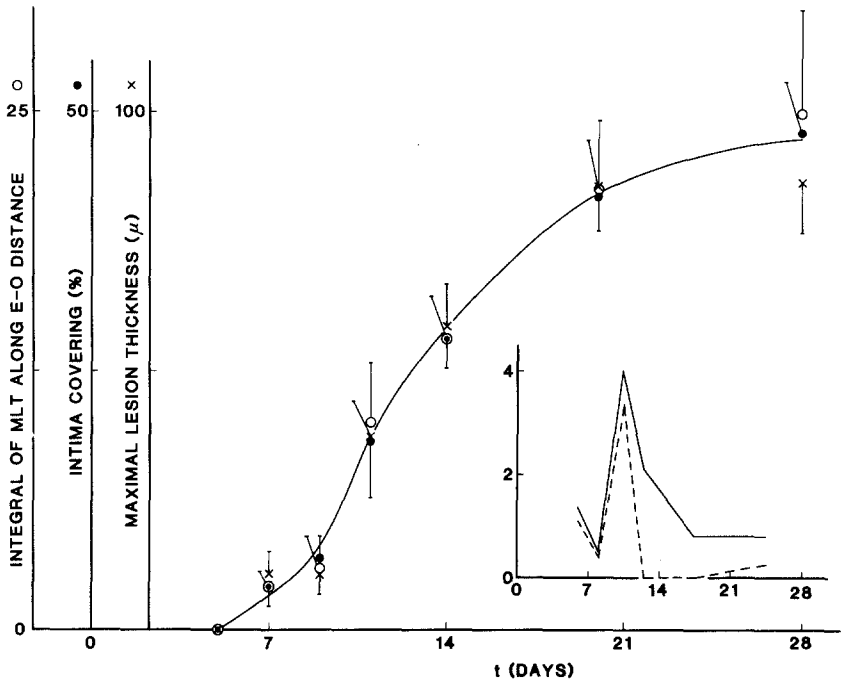

Fig. 6a–c. Characteristics of myointimal thickening in Wi rat carotid artery after air-drying induced endothelial denudation during 28 days after injury (X-axis). The following parameters describing lesion size are scaled on the Y-axis according to their position at day 14. **a** Integral of MLT values at 0.5 mm intervals (o). This parameter describes the surface filled by the pattern of MLT values and the X-axis (cf. Fig. 5). **b** % intima covering (•). This parameter describes the fraction of the intima in which myointimal cells are present. **c** Maximal lesion thickness (MLT) (x). This parameter describes the thickest point of the lesion, whatever its position. Data are given as mean ± SEM. The *inset* represents the changes in myointimal lesion size and media repair in each time sampling interval: (———) $\Delta I/\Delta t$ (changes in the integral of MLT-values along the EO distance); (– – – –) $\Delta M/\Delta t$ (changes in the % of necrosis in the entire media; as repair in the inner and outer medial layers is quite similar, $\Delta M/\Delta t$ represents the mean changes in those layers)

ences in the thickness of the platelet layer have been observed. Axial repair of the endothelium is completed within 21 days. Local areas of incomplete repair (on the thickest parts of the myointimal lesions) remained present in 3 out of 13 animals at day 28. These areas also remained permeable to Evans Blue in 6 out of 13 animals (cf. Fig. 5 X-axis). Rats showing platelet adherence and/or Evans Blue permeation at day 21 or 28 cannot be distinguished from the other rats on the basis of variables describing lesion size.

At day 14, two animals showed a small non-organized thrombus on the still denuded part of the vessel wall. In all other respects, these animals proved indistinguishable from the other animals.

Myointimal lesion development (Figs. 5, 6)

Between days 5 and 7 after endothelial denudation, myointimal cells appear in the intima close to the entrance point of air. Only small amounts of

extracellular matrix can be seen at this stage. Outer medial necrosis is almost absent beneath the developing lesion. Necrosis of the inner medial layer, however, is as extensive here as in the other parts of the vessel wall. The lesion size slightly enlarges up to day 9 and remains at the same site.

The greatest increase in lesion size occurs between days 9 and 11 (cf. inset Fig. 6). During this period, the distal part of the intima also becomes populated with myointimal cells, which can now be found along the entire vessel segment. Lesion thickness is maximum at 1/4 and 3/4 of the EO distance. The mid part of the vessel wall, which is still incompletely re-endothelialized, shows the least myointimal thickening (as well as the most extensive necrosis in both the inner and outer medial layers). Although the myointimal lesion mass continues to increase up to day 28, its growth rate diminishes: at day 14, it is 50% and at later stages 20% of the growth rate measured between days 9 and 11 (cf. Fig. 6 inset). Most of the changes in the myointimal thickening pattern can be found during this time-span in the middle and proximal regions, myointimal lesion thickness in the distal part of the vessel segment is relatively stable. Whereas the intima is relatively thin at earlier stages, it shows the greatest mean lesion thickness at days 21 and 28. The temporary absence of myointimal cells in the proximity of the inflow hole of air at day 21 is of note.

The various variables describing the myointimal lesion development show a remarkably similar pattern (Fig. 6). In all cases, they describe a sigmoid curve having a lag-phase, a phase of accelerating growth to maximal growth rate, after which the growth rate gradually declines (cf. inset Fig. 6).

Comparison of the vessel wall response to endothelial injury in Wistar and in Sprague Dawley rats (Fig. 7; Tables 1, 2, 3)

Necrosis of the inner medial layer is significantly less in SD rats than in Wi rats at 14 days (Table 2). This difference is also found for the mean pattern of necrosis in the middle of the vessel segment (Fig. 7A). The necrotic area of SD rat carotids is mainly restricted to the middle region of the vessel segment (begin and end points at, respectively, 6.7 ± 0.8 mm and 9.3 ± 0.8 mm from the inflow hole), whereas inner medial necrosis in Wi rats at day 14 begins at 2.4 ± 0.5 mm, i.e., significantly more proximal (*t*-test).

Necrosis of the outer medial layer differs significantly in some aspects between SD and Wi rats (Table 2; Fig. 7B). The lesser amount of necrosis in SD rats only reaches significance when considering grade 1 necrosis and the total percentage of necrosis in comparison with Wi rats at days 14 and 28.

Arteriosclerotic myointimal lesions in SD rats differ significantly from those of Wi rats at day 14, thicker lesions covering a greater area of the carotid artery (Table 3).

With the exception of that part of the vessel wall immediately distal to the inflow hole of air (Fig. 8), lesions of SD rats are significantly thicker

than those of Wi rats at day 14. Although in absolute terms SD lesions at day 14 are even larger than those of Wi rats at day 28, this difference is not significant. Wi rat lesions at day 28 are significantly larger than those at day 14 when considering the percentage of the intima covered, the integral of mean lesion thickness values along the EO distance and the mean thickening pattern in the vessel mid part.

Endothelial repair is significantly slower in SD rats as compared with Wi rats (Table 4), when considering the partly re-endothelialized area. Inspection of the sections showed that this was due mostly to less re-endothelialization on the thickest parts of the myointimal lesion.

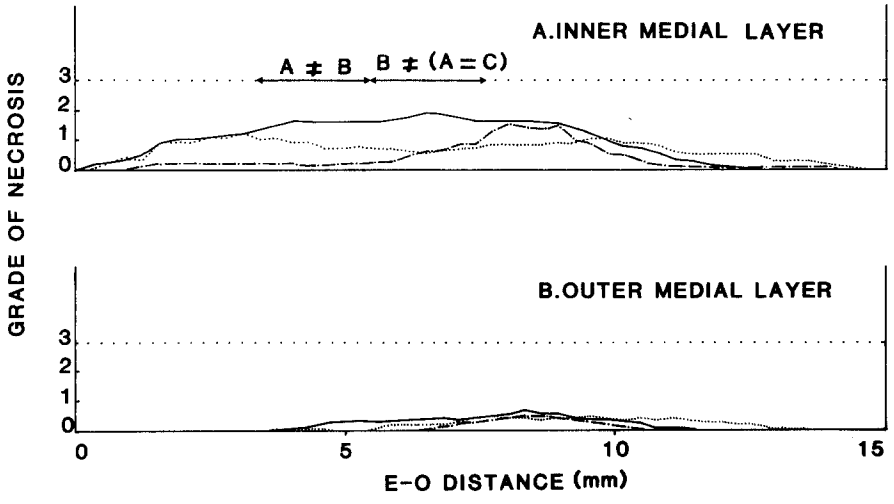

Fig. 7. Graphical representation of the mean grade of medial necrosis of the inner (**A**) and outer (**B**) medial layer(s) along the vessel wall segment denuded of endothelium in Sprague Dawley rats (A;-·—·-) at day 14 after injury and compared with that of Wistar rats at the same time (B;——) and at day 28 after endothelial denudation (C;.....). At *top* of the figures, tests for significant differences using the Kruskall-Wallis test at $\alpha = 0.05$ are indicasted

Table 2. Variables describing necrosis in the inner (i) and outer (o) medial layers in Sprague Dawley rats (day 14 after air-drying injury; A) and Wistar rats (day 14, B and day 28, C, after air-drying injury)

Parameter		SD14 (A)		W14 (B)	
		i	o	i	o
Total % necrosis		12.2±3.7[a]	2.4±1.4	32.3±4.3	7.0±1.9
Length of area (mm), showing necrosis of grade	1	3.0±0.9	0.6±0.3	6.6±0.8	2.2±0.5
	2	1.6±0.4	0.3±0.2	5.1±0.7	0.9±0.3
	3	0.7±0.3	0.1±0.1	3.6±0.6	0.4±0.2

[a] Mean±SEM [b] Tested for significant differences at $\alpha = 0.5$, using ANOVA

Discussion

1. Time course of vessel wall repair

Endothelial regeneration was, in our experiments, somewhat slower than initially described for this model (complete at day 14; Fishman et al. 1975; Clowes et al. 1978) but similar to that described in a later study (Guyton et al. 1980). Newly proliferated endothelial cells overlying myointimal lesions remained partly permeable to Evans Blue. Schwartz et al. (1975) have observed the absence of extensive occluded regions between adjacent cells for up to 6 months after complete de-endothelialization. Therefore, the area of permeability to proteins might be even larger at the submicroscopic level (cf. Clowes 1978).

Regeneration of necrotic media. In this animal model, damage to the media is induced. As has also been described after deep mechanical injury of rabbit aorta (Björkerud and Bondjers 1971), SMCs disappeared from the media within one day, leaving "empty spaces". The media, however, has a great capacity for regeneration (Hassler 1970), provided that the toxic stimulus has not been too strong (Hassler 1970; Björkerud and Bondjers 1971; Spaet et al. 1975). Repair occurs in all layers of the media (Hassler 1970; this study) in axial as well as in circumferential directions. As the rate of repair in the inner and outer media is similar (Table 1; cf. Hassler 1970) this might indicate a comparable reaction to regenerative stimuli throughout the media. The greatest regenerative activity of medial SMCs is found between days 9 and 11. Very probably, a lag-phase of a few days precedes the return of residual SMCs into the Gl-phase. Maximal DNA labeling has been described to precede (Hassler 1970; Burns et al. 1978; Goldberg et al. 1980) the actual increase in cell number (Goldberg et al. 1980), which coincides with maximal activity of other repair processes (endothelial regeneration, myointimal lesion development) in this study. Repopulation of the damaged media has almost ended at day 11, but some repair seems to continue at a low rate up to day 28. Hassler (1970) also describes a continuation of mitotic activity after the media has been injured mechanically or by

W28 (C)		ANOVA[b]			
i	o	i	Ho	o	Ho
22.1±6.8	6.3±3.5	A=C B=C A≠B	0.9	A≠(C=B)	1.5
5.0±1.2	1.6±0.7	A=C B=C A≠B	2.4	A≠(C=B)	0.7
2.7±1.1	0.8±0.5	(A=C) ≠ B	0.3	A=B=C	NS
1.9±1.0	0.4±0.4	(A=C) ≠ B	1.7	A=B=C	NS

Table 3. Variables describing the size and position of myointimal thickening in Sprague Dawley rats at day 14 after air-drying injury (A) and Wistar rats (day 14, B; day 28, C)

Variable		SD14 (A)	W14 (B)	W28 (C)	ANOVA[b]	Ho
Position	Begin (mm)	1.3± 0.4[a]	2.1±0.5	1.7±0.5	A=B=C	NS
	End (mm)	13.4± 0.5	10.8±0.5	12.4±0.6	B=C C=A A≠B	0.6
Size	Length (mm)	12.2± 0.8	8.7±0.6	10.7±0.7	B=C C=A A≠B	0.4
	Maximal thickness (μm)	93.6±10.3	58.8±8.2	85.9±9.6	B=C C=A A≠B	1.8
	Intima covering (%)	51.7± 5.0	28.1±2.9	48.0±4.7	B≠(C=A)	0.01
	Integral of mean lesion thickness along EO-distance	32.2± 4.1	14.1±2.1	24.9±5.0	B≠(C=A)	0.12

[a] Mean±SEM
[b] Tested for significant differences at $\alpha=0.05$, using ANOVA

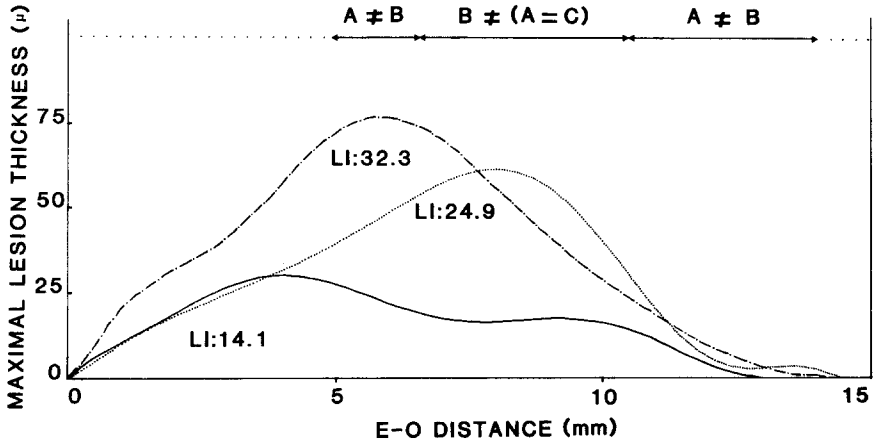

Fig. 8. Myointimal thickening in Sprague Dawley rat carotid artery at day 14 after air-drying (A;–·–·–) and compared with the lesions found in Wistar rats at days 14 (B;——) and 28 (C;.....). These curves were generated in a similar way as described for Fig. 5. At the *top*, tests for significant differences using the Kruskall-Wallis test at $\alpha=0.05$ are indicated

freezing. Whether the media will recover completely cannot be concluded from the present study. Our results for up to day 28 suggest that the state of the media at day 11 (or 14) is aproximately the end point of medial repair. In general, medial repair represents a limited proliferative stimulus.

Myointimal lesion development. Intimal SMCs can first be identified at day 7 (cf. Fishman et al. 1975). Myointimal lesions have been described as appearing at day 7 after longitudinal and/or transverse injury in rat aorta (Bondjers and Björnheden 1970), at day 3–7 in Wistar rat aorta after balloon injury (Schwartz et al. 1975; Haudenschild and Schwartz 1979), at day 4 in Sprague

Table 4. Variables describing endothelial repair in Sprague Dawley (SD) and Wistar (Wi) rats at day 14 after air-drying injury

	SD14	W14	Ho[b]
Begin of fully denuded intima (mm)	5.6±0.4[a]	6.5±0.3	NS
End of fully denuded intima (mm)	8.0±0.5	7.6±0.3	NS
Begin of partly re-endothelialized intima (mm)	4.0±0.5	5.7±0.4	1.5
End of partly re-endothelialized intima (mm)	11.1±0.5	8.8±0.3	0.06
Begin of Evans Blue permeation (mm)	5.3±0.6	4.3±0.4	NS
End of Evans Blue permeation (mm)	10.9±0.9	8.7±0.4	1.3

Students *t*-test was used

[a] Mean±SEM
[b] Students *t*-test

Dawley rat carotid artery after air-drying injury (Clowes et al. 1978), and at day 3–7 in rabbits (Goldberg et al. 1980).

During the initial stages of myointimal lesion development, neointimal cells are primarily found in the proximity of the inflow hole of air, possibly because mitogenic and/or chemotactic factors (e.g., platelet-derived growth factor) are in higher concentration at that point (Thorgeirsson et al. 1979; Ross 1981; Grotendorst et al. 1982), while mitogenic factors for SMCs such as thrombin and fibrin (Bruhn 1981; Ishida and Tanaka 1982) are also generated during haemostasis at the puncture hole. After day 9, myointimal lesion development occurs along the entire denuded segment (Burns et al. 1978).

At day 28, lesions are considerably thicker than at day 14 (cf. Guyton et al. 1980). They have therefore continued to grow after day 14, as was also described by Tiell et al. (1982), Koletsky and Snajdar (1981), in contrast to earlier data (Fishman et al. 1975; Clowes et al. 1976, 1978).

The time pattern of myointimal lesion growth rate, showing peak values between days 9 and 11, followed by a decline, resembles that of rabbit abdominal aorta after balloon catherization (Goldberg et al. 1980).

2. The effect of medial necrosis on myointimal lesion development

As medial necrosis might diminish the pool of SMCs available for proliferation and migration into the intima, we wondered whether it influenced lesion development. Between groups of Wistar rats (air-flow rate studies), differences in necrosis did not give rise to differences in myointimal lesion size at one time point. We suggested previously that lesion development is the result of mitogenic and chemotactic factors in intima and media, on which was superimposed an effect of medial necrosis (van Pelt-Verkuil et al. 1983). The present study may illustrate the effect of medial necrosis within a given experimental group of Wi rats on local myointimal lesion development. At day 9, selective lesion development at the inflow hole is

accompanied by little outer medial necrosis at the site. During the phase of most extensive SMC proliferation in intima and media (day 9–11), mean lesion thickness values are found to be smallest at the location showing the most severe inner and outer medial necrosis (the vessel midpart). As only a starting pool of SMCs seems to originate from the media, which pool subsequently proliferates in the intima itself (Burns 1978), we might see in this study the effects of local shortage of the initial pool of intimal SMCs due to medial necrosis. In this context, the greater lesions of SD rats might be explained by a greater pool of SMCs available in the less damaged SD media.

3. Interstrain differences

Strain differences in the vessel wall reaction to noxious stimuli and in spontaneous atherosclerosis have been observed before (Wagner et al. 1973; Subbiah 1976).

Spontaneously hypertensive rats show a much stronger response to endothelial denudation of the carotid artery than do other rat strains (Koletski and Snajdar 1981; Clowes and Clowes 1980).

For the observed differences between SD and Wi rats with respect to myointimal lesion development, media necrosis and endothelial repair, several explanations can be suggested. Firstly, if medial SMCs of SD rats show a higher proliferative capacity, similar initial necrosis will result in larger lesions as compared with Wi rats. SD rats might be more sensitive to mitogenic factors, as has been suggested for spontaneously hypertensive rats by Clowes and Clowes (1980). SMCs of the latter strain have been reported to be more prone to proliferate in aorta explants than those of Wistar rats (Yamori et al. 1981). It is also possible that, if medial SMCs of SD rats have a similar proliferation capacity, the larger lesions in SD rats might be due to the availability of more SMCs for migration into the intima to form the starting pool of SMCs, due to less media necrosis, or to a higher initial cellular density. Secondly, larger amounts of growth factors might reach the media when endothelial repair is slow. Endothelial repair in SD rats is slower in all aspects measured, as has also been reported for hypertensive rats denuded of endothelium (Clowes et al. 1978; Clowes and Clowes 1980). This will prolong the period during which the underlying vessel wall is exposed to growth factors from the blood, e.g., pituitary-derived growth factor (Tiell et al. 1978). Finally, the blood and/or vessel wall might be more thrombogenic in SD rats. SD rats are more thrombogenic in aortic loop experiments than are Wistar rats (Lecker and Kumar 1980). More platelet and/or fibrin deposition at the denuded intima might generate more mitogenic and/or chemotactic factors.

Our present state of knowledge does not allow us to prefer one or more of these possibilities. We hypothesize, however, that a comination of longer denudation of the intima, allowing more growth factors from the blood to reach the intima, of less damage to the media and of a greater initial

mitogenic stimulus (more platelet factors and fibrin generated during the initial stages) might cause the larger myointimal lesions in SD rats.

References

Björkerud S, Bondjers G (1971) Arterial repair and atherosclerosis after mechanical injury. Part 2. Tissue response after induction of a total local necrosis (deep longitudinal injury). Atherosclerosis 14:259–276

Björkerud S, Bondjers G (1973) Arterial repair and atherosclerosis after mechanical injury. Part 5. Tissue response after induction of a large superficial transversal injury. Atherosclerosis 18:235–255

Bondjers G, Björnheden T (1970) Experimental atherosclerosis induced by mechanical trauma in rats. Atherosclerosis 12:301–306

Bruhn HD (1981) Growth regulation of vessel wall cells and of tumor cells by thrombin, Factor XIII and fibronectin.Thromb Haemost 46:762

Burns ER, Spaet TH, Stemerman MB (1978) Response of the arterial wall to endothelial removal: an autoradiographic study. Proc Soc Exp Biol Med 159:473–477

Clowes AW, Clowes MM (1980) The influence of hypertension on injury-induced myointimal thickening. Surgery 88:254–259

Clowes AW, Ryan GB, Breslow JL, Karnovsky MJ (1976) Absence of enhanced intimal thickening in the response of the carotid arterial wall to endothelial injury in hypercholesterolemic rats. Lab Invest 35:6–16

Clowes AW, Callazzo RE, Karnovsky MJ (1978) A morphologic and permeability study of luminal smooth muscle cells after arterial injury in the rat. Lab Invest 39:141–150

Falcone DJ, Hajjar DP, Minick CR (1980) Enhancement of cholesterol and cholesterylester accumulation in re-endothelialized aorta. Am J Pathol 99:81–104

Fishman JA, Ryan GB, Karnovsky MJ (1975) Endothelial regeneration in the rat carotid artery and the significance of endothelial denudation in the pathogenesis of myointimal thickening. Lab Invest 32:339–351

Goldberg ID, Stemerman MD, Ransil BJ, Fuhra RL (1980) In vivo aortic muscle cell growth kinetics. Differences between thoracic and abdominal segments after intimal injury in the rabbit. Circ Res 47:182–189

Grotendorst GR, Chang T, Seppä HEJ, Kleinman HK, Martin GR (1982) Platelet derived growth factor is a chemoattractant for vascular smooth muscle cells. J Cell Physiol 113:261–266

Guyton JR, Rosenberg RD, Clowes AW, Karnovsky MJ (1980) Inhibition of rat arterial smooth muscle cell proliferation by heparin. In vivo studies with anticoagulant and non-anticoagulant heparin. Circ Res 46:625–634

Hassler O (1970) The origin of the cells constituting arterial intima thickening. An experimental autoradiographic study with the use of H^3-thymidine. Lab Invest 22:286–293

Haudenschild CC, Schwartz SM (1979) Endothelial regeneration. II Restitution of endothelial continuity. Lab Invest 41:407–418

Haudenschild CC, Van Sickle W, Chobanian AV (1981) Response of the aorta of the obese Zucker rat to injury. Arteriosclerosis 1:186–191

Hirsch EZ, Robertson AL (1977) Selective acute arterial endothelial injury and repair. I Methodology and surface characteristics. Atherosclerosis 28:271–287

Ishida T, Tanaka K (1982) Effects of fibrin and fibrinogen degradation products on the growth of rabbit aortic smooth muscle cells in culture. Atherosclerosis 44:161–174

Karnovsky MJ (1981) Endothelial-vascular smooth muscle cell interactions. Am J Pathol 105:200–206

Koletski S, Snajdar RM (1981) Atherosclerosis following balloon catheter injury to the carotid artery and the aorta of hypertensive rats with normolipidemia or hyperlipidemia. Am J Pathol 103:105–115

Lecker D, Kumar A (1980) Effects of 6-(p-(4-phenyl acetylpiperazin-L-yl)-phenyl)-4.5-dinitro-3(2H7-pyridazinone (CCI 17810) and aspirin on experimental arterial thrombosis in rats. Thromb Haemost 44:9–11

Van Pelt-Verkuil E, Van Pelt W, Jense D (1983) Morphometry of air-drying induced arteriosclerosis in rat carotid artery: the effect of the air-flow rate. Arteriosclerosis 3:441–451

Poole JCF, Cromwell SB, Benditt EP (1971) Behavior of smooth muscle cells and formation of extracellular structures in the reaction of arterial walls to injury. Am J Pathol 62:391–413

Reidy MA, Standaert D, Schwartz SM (1982) Inhibition of endothelial cell regrowth. Cessation of aortic endothelial cell replication after balloon catheter denudation. Arteriosclerosis 2:216–220

Ross R (1981) Atherosclerosis: a problem of the biology of arterial wall cells and their interactions with blood components. Arteriosclerosis 1:293–311

Ross R, Glomset J (1973) Atherosclerosis and the arterial smooth muscle cell. Science 180:1332–1339

Ross R, Glomset J (1976) The pathogenesis of atherosclerosis. N Engl J Med 295:369–377; 420–425

Schwartz SM, Stemerman MB, Benditt EP (1975) The aortic intima. II Repair of the arotic lining after mechanical denudation. Am J Pathol 81:15–42

Spaet TH, Stemerman MB, Veith FJ, Lejnieks I (1975) Intimal injury of neointima. Circ Res 36:58–70

Subbiah MTR (1976) White Carneau pigeon: an ideal model for the study of progression and regression of atherosclerosis. Biochem Exp Biol 12:229–234

Thorgeirsson G, Robertson AL (1978) The vascular endothelium – Pathobiologic significance. Am J Pathol 93:802–848

Thorgeirsson G, Robertson AL, Cowan DH (1979) Migration of human vascular endothelial and smooth muscle cells. Lab Invest 41:51–62

Tiell ML, Stemerman MB, Spaet TH (1978) The influence of the pituitary on arterial intimal proliferation in the rat. Circ Res 42:644–649

Tiell ML, Sussman II, Moss R, Drouet LC, Spaet TH (1982) Production of experimental arteriosclerosis in Fawn-Hooded rats with platelet storage pool deficincy. Artery 10:329–340

Wagner WD, Clarkson TB, Feldner MA, Prichard RW (1973) The development of pigeon strains with selected atherosclerosis characteristics. Exp Mol Pathol 19:304–319

Yamori Y, Igawa T, Kanbe T, Kihara M, Nara Y, Horie R (1981) Mechanisms of structural vascular changes in genetic hypertension: analyses on cultured vascular smooth muscle cells from spontaneous hypertensive rats. Clin Sci 61:121S–123S

Accepted November 1, 1985